

The circadian mutation *PER2*^{S662G} is linked to cell cycle progression and tumorigenesis

X Gu^{1,3}, L Xing^{1,3}, G Shi¹, Z Liu¹, X Wang¹, Z Qu¹, X Wu¹, Z Dong¹, X Gao¹, G Liu¹, L Yang^{*2} and Y Xu^{*1}

Circadian oscillation and cell cycle progression are the two most essential rhythmic events present in almost all organisms. Circadian rhythms keep track of time and provide temporal regulation with a period of about 24 h. The cell cycle is optimized for growth and division, but not for time keeping. Circadian gated cell divisions are observed in nearly all organisms. However, the implications of this coupling to the physiology of mammals are unknown. A mutation (S662G) in the clock protein PERIOD2 (PER2) is responsible for familial advanced sleep phase syndrome in which sleep onset occurs in the early evening and wakefulness occurs in the early morning. Here, we provide evidence that the *PER2*^{S662} mutation leads to enhanced resistance to X-ray-induced apoptosis and increased E1A- and RAS-mediated oncogenic transformation. Accordingly, the *PER2*^{S662} mutation affects tumorigenesis in cancer-sensitized *p53*^{R172H/+} mice. Finally, analyzing the clock-controlled cell cycle genes *p21*, *c-Myc*, *Cyclin D1* and *p27*, we found that the relative phases between *p21* and *Cyclin D* expression profiles have been changed significantly in these *Per2* allele mutant mouse embryonic fibroblasts. This key role of the *Per2*-mediated phase alteration of *p21* provides what we believe to be a novel mechanism in understanding cell cycle progression, its plasticity and its resistance to interference.

Cell Death and Differentiation (2012) 19, 397–405; doi:10.1038/cdd.2011.103; published online 5 August 2011

The circadian clock is essential for the maintenance of physiological homeostasis, as well as the coordination of responses to external signals. In mammals, the circadian clock is composed of interlocking positive and negative feedback loops. In the primary feedback loop, three basic helix–loop–helix (bHLH)/PAS domain-containing transcription factors, *Clock*, *Npas2* and *Bmal1*, activate the transcription of two period genes (*Per1* and *Per2*) and two cryptochrome (*Cry*) genes (*Cry1* and *Cry2*) by binding to the E-box *cis* elements in the promoters of these genes. Subsequently, the PER/CRY complex inhibits the transcription of its own genes by blocking BMAL1/CLOCK activity. The second feedback loop is mediated by the orphan nuclear receptors ROR α and Rev-erb α . Transcription of *ROR\alpha* and *Rev-erba* is activated during the day by the CLOCK/BMAL1 complex, after which they exert positive and negative transcriptional effects on the *Bmal1* gene through Rev-erb α /ROR α responsive elements (ROREs) in the *Bmal1* promoter.^{1–3} The circadian system may be tightly connected to many physiological processes through clock-controlled nuclear receptor genes (e.g., PPAR α and PPAR γ) and cell cycle genes (e.g., *c-Myc*, *cyclin D*, *Wee1* and *p21*).^{5–8} The links between the circadian clock and a variety of physiological processes are just beginning to be unveiled; however, the underlying mechanisms remain unclear.

A major consequence of a modern lifestyle is the disruption of circadian rhythms. Importantly, epidemiological studies have shown that a disruption in circadian rhythms increases an individual's risk of developing colon, breast, prostate, ovarian, lung and liver cancer.^{9,10} The International Agency for Research on Cancer has elevated the carcinogenicity of circadian disruption from Group 2B to Group 2A.¹¹ Furthermore, several studies using mouse models have established convincing links between mutations in certain clock genes and tumorigenesis. Targeted disruption of PERIOD2 (*Per2*) leads to tumor susceptibility in the presence of γ radiation.⁶ *Per1* also functions as a tumor suppressor by regulating cell cycle genes and by interacting with key checkpoint proteins that are activated by DNA damage.⁸ Given the strong links between circadian rhythms and the diverse physiological processes in these animal models, it is important to address whether human circadian variations influence cancer susceptibility.

Advanced sleep phase syndrome (ASPS) is a circadian rhythm variant in which sleep onset occurs in the early evening (i.e., 1800–2000 hours) and, as a consequence, wakefulness occurs in the early morning (i.e., 0100–0300 h).^{12–14} The discovery that the *PER2*^{S662G} mutation causes familial ASPS (FASPS) was the first direct evidence that PER2 has an essential role in the human circadian

¹MOE Key Laboratory of Model Animal for Disease Study, Model Animal Research Center, Nanjing University, Nanjing, China and ²Center for Systems Biology, Soochow University, Soochow, China

*Corresponding author: L. Yang, Center for Systems Biology, Soochow University, Soochow 215006, China. Tel: +86 512 65112418; Fax: +86 512 65110951; E-mail: lyang@suda.edu.cn

or Y Xu, MOE Key Laboratory of Model Animal for Disease Study, Model Animal Research Center, Nanjing University, 12 Xuefu lu, Pukou District, Nanjing 210061, China. Tel: +86 25 58641504; Fax: +86 25 58641500; E-mail: yingxu@nju.edu.cn

³These two authors contributed equally to this work.

Keywords: PER2; circadian rhythms; cell cycle; tumorigenesis; FASPS

Abbreviations: PER2, PERIOD2; FASPS, familial advanced sleep phase syndrome; ASPS, advanced sleep phase syndrome; ZT, Zeitgeber Time; MEF, mouse embryonic fibroblast; KO, knockout; BAC, bacterial artificial chromosome; ANOVA, one-way analysis of variance; RT-PCR, reverse transcription PCR; RORE, Rev-erb α /ROR α responsive elements; Cry, cryptochrome

Received 08.4.11; revised 27.6.11; accepted 30.6.11; Edited by C Borner; published online 05.8.11

clock.^{13,15} Furthermore, given that this specific amino acid of the PER2 protein may represent an appealing therapeutic target, we investigated whether the S662 site is also crucial for its function as a tumor suppressor. Moreover, *PER2*^{S662G} and *PER2*^{S662D} transgenic mice are unique because single amino-acid changes at this site can either shorten or lengthen the circadian period in a mutation-dependent manner, thus providing a unique model to understand how circadian period length affects cell cycle progression and tumorigenesis.

In the present study, we focused on characterizing the link between *PER2*^{S662} mutations and tumorigenesis both *in vitro* and *in vivo*. We found that mutation of *PER2*^{S662} affects tumorigenesis in *p53*^{R172H/+} mice, which have a cancer-sensitized genetic background caused by a p53 knock-in mutation^{2H,16}. We subsequently found that PER2 acts as a phase regulator, directly or indirectly, to affect the advanced or delayed cell cycle gene expression profiles, but not amplitude. These findings raise the possibility that alteration of *p21* phase by *Per2* allele mutant may interfere with cell phase locking to promote cell cycle progression.

Results

S662 is a key amino acid in PER2 that modulates X-ray-induced apoptosis. We first investigated whether S662 in PER2 is crucial for its function as a tumor suppressor by analyzing the apoptotic response. To avoid potential interference from the wild-type *Per2* gene, we crossed both *PER2*^{S662G} and *PER2*^{S662D} (amino acid 662 changed from serine to aspartate) bacterial artificial chromosome (BAC) transgenic mice to a *Per2*^{-/-} background.^{15,17} The resultant compound mice, aged 8–10 weeks, were treated with 6-Gy X-ray irradiation at Zeitgeber Time (ZT) 0 and ZT 9. The percentage of apoptotic spleen cells was reduced significantly (approximately two fold) in *Per2*^{-/-} spleens compared with those of wild-type littermates at ZT 0 and ZT 9, as shown by flow cytometry (Figures 1a and b). Interestingly, the cells from *PER2*^{S662G}.*Per2*^{-/-} mice displayed markedly attenuated levels of apoptosis that were similar to those of *Per2*^{-/-} mice, and *PER2*^{S662D}.*Per2*^{-/-} mice were even more resistant to X-ray-induced apoptosis than *Per2* knockout (KO) mice (Figure 1b).

Generation of *PER2* dose-dependent BAC transgenic mice. As there is a higher level of PER2 in *PER2*^{S662D} mice compared with wild-type littermates,¹⁵ it is plausible that PER2 may affect apoptosis through multiple mechanisms. To determine whether increased expression of PER2 compared with wild-type levels is also responsible for the observed resistance to apoptosis, we generated *PER2* dose-dependent BAC transgenic mice (Figure 2a). These transgenic mice were designed to express *cis*-acting genomic regulatory elements in a manner that faithfully recapitulates endogenous *PER2* expression. We characterized these mice based on their copy number by Southern blot (Figure 2b) and quantitative-PCR (Q-PCR) (Figure 2c), and then we selected three transgenic lines as low (1–2 copies) (L), middle (2–3 copies) (M) and high copy

(4–5 copies) (H). mRNA levels are much higher in the H line than in the *PER2*^{S662D/2H} in including liver (Figure 2d), spleen (Figure 2e) and mouse embryonic fibroblasts (MEFs) (Figure 2f), and PER2 protein in H line is more abundant than those from the *PER2*^{S662D} mice (Figure 2g). These mice have a circadian period that lengthens as the copy number of *Per2* increases (Figure 2h). Mice with four to five copies of the *PER2* transgene showed an extreme elongation of the circadian period to 25 h, which is longer than that of the mice with the *PER2*^{S662D} mutation (24 h).¹⁵ The PER2 dose dependence of period length suggests that PER2 has a critical role in circadian clock, which is also seen in *drosophila*.^{18,19} *PER2*^{S662D} may elongate the circadian period through the increased PER2 protein level. We noticed that apoptosis rates also decreased in the high-copy mice (28% ± 0.9), but this decrease is less than that in the *PER2*^{S662G}.*Per2*^{-/-} mutant (16.5% ± 0.3), *PER2*^{S662D}.*Per2*^{-/-} mutant (9.9% ± 0.05) and *Per2*^{-/-} mice (15.08% ± 0.2) ($P < 0.001$) (Figures 3a and b). This suggests that PER2 homeostasis has a role in maintaining a proper apoptosis response. Furthermore, we crossed L-line mice to the *Per2*^{-/-} background because all results are on a *Per2*^{-/-} background. The cells from L-line mice displayed comparable levels of apoptosis to those from L line on a *Per2*^{-/-} background (35.1 ± 0.1 versus 35.2 ± 0.5), to exclude a remote possibility that *Per2*^{-/-} acts as a dominant negative role. These genetic observations suggest that both the mutational status of *PER2*^{S662} and the levels of PER2 protein may affect the apoptotic response to X-rays.

Mutation of S662 promotes oncogenic E1A-RAS-induced transformation in MEFs. A previous study has shown that primary embryo fibroblasts can be immortalized by the expression of at least two oncogenes; for example, *E1A*, *myc* and *ras*.²⁰ This technique has been used to evaluate whether inactivation or deletion of a tumor suppressor gene can hasten the activation of oncogenes and promote oncogenic transformation.²¹ To determine whether the *PER2*^{S662} mutation results in a transformation-permissive phenotype *in vitro*, *PER2*^{S662G}, *PER2*^{S662D}, wild-type and *Per2*^{-/-} MEFs were infected with a retroviral vector that co-expressed the oncogenes *E1a* and *Ras*. The ability of *E1a* and *Ras* to induce cellular transformation was far greater in *PER2*^{S662G} mice than in wild-type MEFs, while the level of transformation was comparable to that of *Per2* KO MEFs (Figures 4a and b). Furthermore, consistent with the phenotype shown for X-ray-induced apoptosis, *PER2*^{S662D} MEFs formed more colonies than *PER2*^{S662G} and *Per2*^{-/-} MEFs (Figures 4a and b). Finally, we assessed whether overexpression of wild-type *PER2* could trigger cellular transformation. As expected, the MEFs with a high-copy number of *Per2* from H line grew more colonies than those with a low-copy number of *Per2* or wild-type MEFs, but they grew fewer colonies than *PER2*^{S662D} mutant MEFs (Figures 4c and d). The numbers for *E1a*- and *Ras*-induced transformation foci are 310 ± 107 for *PER2*^{S662D}, 205 ± 52 for H line, 158 ± 25 for *Per2*^{-/-}, 150 ± 36 for *PER2*^{S662G}, 96 ± 24 for L line, 74 ± 35 for wild type and 8 ± 5 for no-transfection control. These mice are on a wild-type background because of technical difficulty getting all embryos from seven

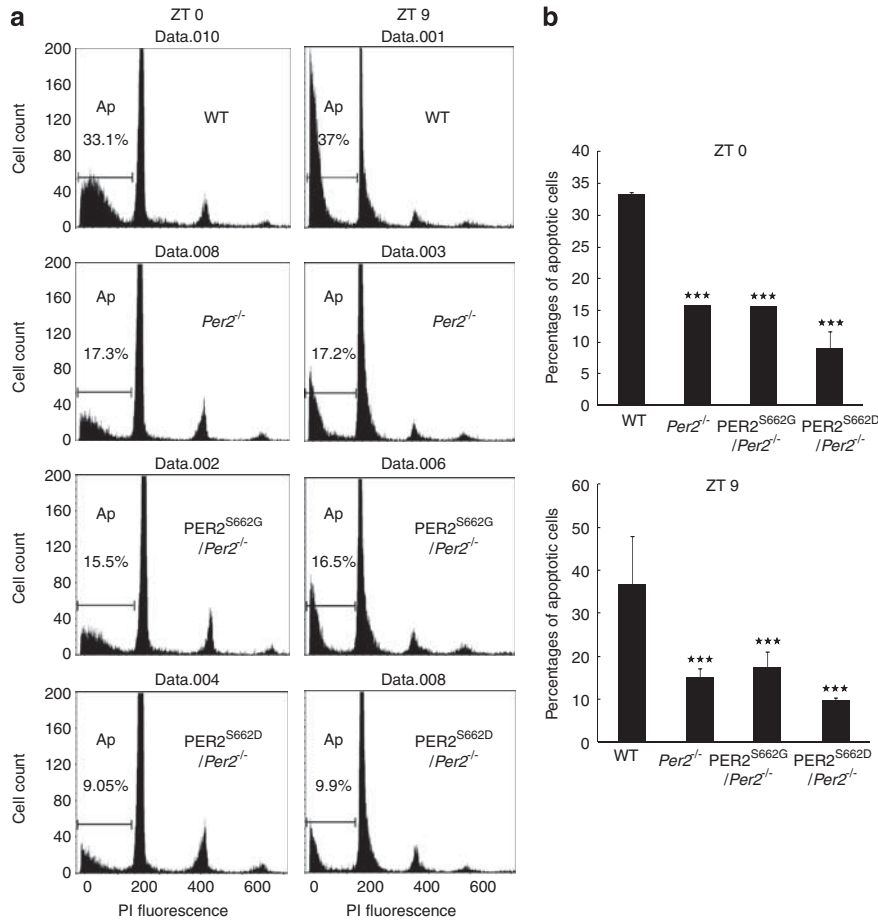


Figure 1 The *PER2*^{S662} mutation leads to decreased levels of apoptosis. **(a)** Wild-type, *Per2*^{-/-}, *PER2*^{S662G};*Per2*^{-/-} and *PER2*^{S662D};*Per2*^{-/-} mice were irradiated with 6 Gy X-rays at ZT 0 (0800 hours) and ZT 9 (1700 hours). Spleen cells were isolated 6 h after irradiation, stained with propidium iodide (PI) and analyzed by flow cytometry. One representative experiment is shown. Ap, apoptotic percentage. **(b)** Percentages of apoptotic cells measured by flow cytometry are shown in the histograms. Experiments were repeated at least three times with consistent results and at least two mice were used per group for each time (*N*=3 for each genotype; ****P*<0.001; one-way ANOVA followed by Dunnett's test)

genotype mice on a *Per2*^{-/-} background at one time. These findings are consistent with the apoptotic responses observed after X-ray exposure. Furthermore, similar transformation rates between *PER2*^{S662G} on wild-type background and *Per2*^{-/-}MEFs suggest that *PER2*^{S662G} is not just a loss of function mutation but has a dominant role. Altogether, these results illustrate the importance of the S662 site and of maintaining an appropriate level of PER2 to mediate the cellular response to environmental mutagens.

Mutations in *PER2*^{S662} accelerate tumorigenesis in *p53*^{R172H/+} background mice. The influence of *PER2*^{S662} mutations on both X-ray-induced apoptosis and *in vitro* transformation led us to assess the relevance of the *PER2*^{S662} mutation with regard to tumorigenesis *in vivo*. It has been noted that a mutation in one or more core clock genes is not sufficient to elicit increased tumor incidence in the absence of a cancer-sensitized genetic background.²²

As the *PER2*^{S662} mutation is found in a human circadian variant, we mated *PER2*^{S662} mutant mice with *p53*^{R172H} knock-in mice. These knock-in mice have a mutation

that corresponds to the *p53*^{R175H} hot spot in human cancers.¹⁶ Through breeding, we established cohorts of *p53*^{R172H/+} (*n*=54), *PER2*^{S662G2H};*p53*^{R172H/+} (*n*=41), *PER2*^{S662D2H};*p53*^{R172H/+} (*n*=31) and *Clock*^{Δ19/+};*p53*^{R172H/+} (*n*=29) compound mutant mice. These mice all had the same genetic background of C57BL/6. We monitored these mice for tumor development and survival for up to 700 days. As shown in Figure 5a, Kaplan–Meier overall survival curves of these compound mutant mice showed slight but significant differences (log-rank test, *P*=0.049). A closer inspection of the data revealed that the survival of female *p53*^{R172H/+} and *Clock*^{Δ19/+};*p53*^{R172H/+} mice was decreased markedly compared with that of male mice (Supplementary Figures S1A and B). But the survival of *PER2*^{S662G2H};*p53*^{R172H/+} and *PER2*^{S662D2H};*p53*^{R172H/+} mice did not show any gender-based differences (Supplementary Figures S1C and 1D). Thus, to further dissociate the effects of the *PER2*^{S662} mutation on tumor development, we assessed male and female survival curves separately. The survival curve for males was significantly affected by circadian gene mutations (Figure 5b, log-rank test, *P*<0.001). The median life spans

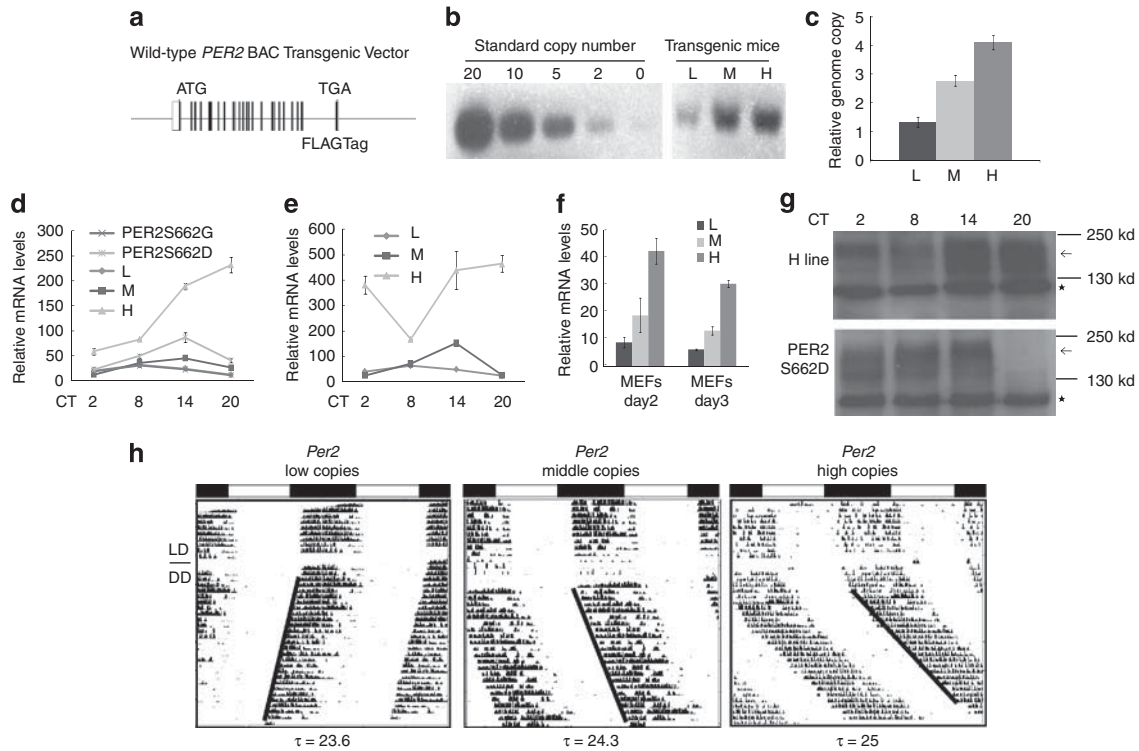


Figure 2 Generation and characterization of *PER2* BAC transgenic mice. (a) Generation of different copy BAC transgenic mice. (b) Transgene copy number was estimated by Southern blot by comparing with copy standards. Experiments were repeated two times with consistent results and one mouse was used per line. (c) The relative transgene copy number was further estimated by q-PCR. (d–f) The mRNA expression level was assessed by qRT-PCR in liver tissues (d), spleen tissues (e) and non-synchronized MEFs (f) of different BAC transgenic mice as indicated genotypes. Experiments were repeated independently at least three times with consistent results and at least two replicates were used per time point. ‘→’ denotes the band of *PER2* and ‘*’ denotes a unspecific band. (g) *PER2* protein levels in spleen tissues of H line and *PER2*^{S662D}. Experiments were repeated three times with consistent results, and one mouse for each time point was used for western blot. (h) Voluntary locomotor activities were recorded as wheel-running activity. BAC transgenic mice were subjected first to LD (light and dark cycle) and then released into DD (dark and dark cycle). Representative actograms from low- (23.64 ± 0.11, n = 6), middle- (24.34 ± 0.18, n = 7) and high-copy BAC transgenic mice (25.07 ± 0.17, n = 9). Alternating white and dark bars indicate the LD cycles during entrainment before release in DD

were also reduced for male *PER2*^{S662D2H}.*p53*^{R172H/+} (15.0 months) and *PER2*^{S662G2H}.*p53*^{R172H/+} (16.6 months) mice compared with those of male *p53*^{R172H/+} (17.9 months) and *Clock*^{Δ19/+}.*p53*^{R172H/+} (19.8 months) mice (Figure 5b). As tumors in *p53*^{R172H/+} mice arise after a similar length of latency, these differences in the survival curves and median life spans reflected changes that contributed to tumorigenesis.

This raises the question of why female and male on a *p53*^{R172H/+} background have different survival rates, and why we did not observe a difference between *PER2*^{S6622H}.*p53*^{R172H/+} and *p53*^{R172H/+} female mice, in contrast to the male mice. Of note, we did not obtain any *p53*^{R172H/R172H} female homozygous mice from 75 pups (Supplementary Table 1), and we found that they all died by 13.5 days as a result of fatal embryonic exencephaly (Figure 6). These findings are consistent with a previous reporting that lack of the tumor suppressor protein p53 causes a female-specific disruption of neural tube closure associated with embryonic or neonatal death.²³ This suggests that female *p53*^{R172H/+} mice may have a penetrant phenotype that could have masked the effects of *PER2*^{S662} mutations on female tumorigenesis. These data demonstrate collectively that the *PER2*^{S662} mutation has an impact on tumor development in the *p53*^{R172H/+} mutant background.

Circadian cycle length is not tightly associated with tumorigenesis. Then, we tested whether the accelerated tumorigenesis caused by *PER2*^{S662} mutation was related to the alteration in circadian period. As shown in Supplementary Figures 2A and B, the *p53*^{R172H/+} mutation did not affect the circadian period or the expression of core clock genes. Furthermore, in the *PER2*^{S662G2H}.*p53*^{R172H/+}, *PER2*^{S662D2H}.*p53*^{R172H/+} and *Clock*^{Δ19/+}.*p53*^{R172H/+} mice, circadian period was not closely related to tumor development (Figure 5a and Supplementary Figure S2C).

The most common tumor types observed in mice of the above genotypes are lymphomas and sarcomas, consistent with the reported tumor ratio of *p53*^{R172H/+} mice (Supplementary Figure S3).¹⁶ It is noteworthy that the incidence of primary hepatic malignancy and metastatic tumors was increased in *PER2*^{S662G2H}.*p53*^{R172H/+} (27.3%) and *PER2*^{S662D2H}.*p53*^{R172H/+} mice (19.4%) compared with that in *p53*^{R172H/+} mice (8.7%), although it did not reach statistical significance ($P = 0.17$) (Table 1). We observed that circadian cycle length was also not associated with certain types of tumors (Table 1). These results support the notion that mutation of *PER2* at S662 promotes tumorigenesis, independent of the acceleration or deceleration of the circadian clock.

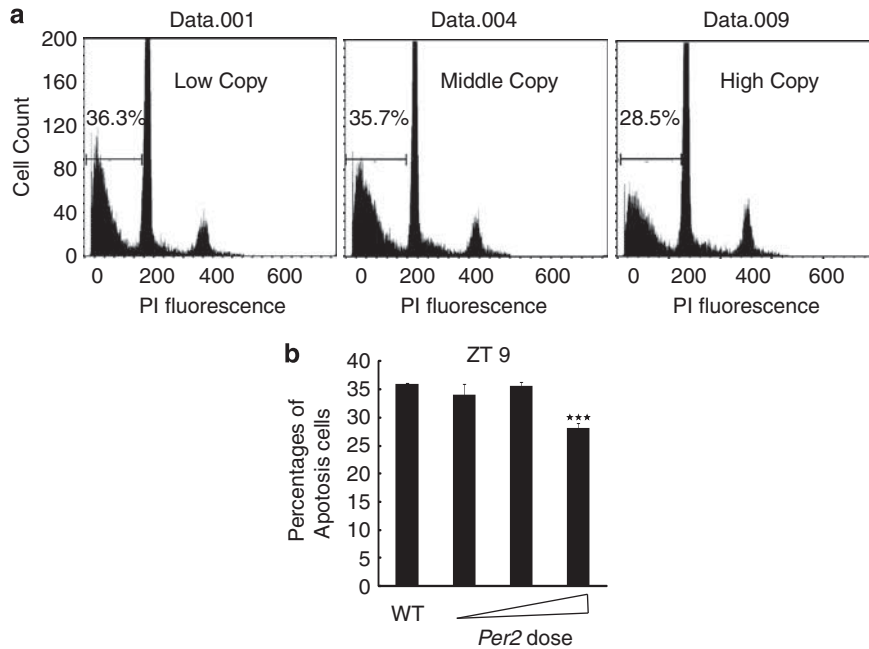


Figure 3 High-dose *PER2* results in resistance to apoptosis induced by X-rays. (a) Low-, middle- and high-copy *PER2* mice were irradiated with 6 Gy X-rays at ZT 9. Spleen cells were isolated 6 h after irradiation and the DNA content was analyzed by flow cytometry. One representative experiment is shown. (b) Percentages of apoptotic cells detected by flow cytometry from low-, middle- and high-copy BAC transgenic spleens (***) $P < 0.001$; one-way ANOVA followed by Dunnett's test)

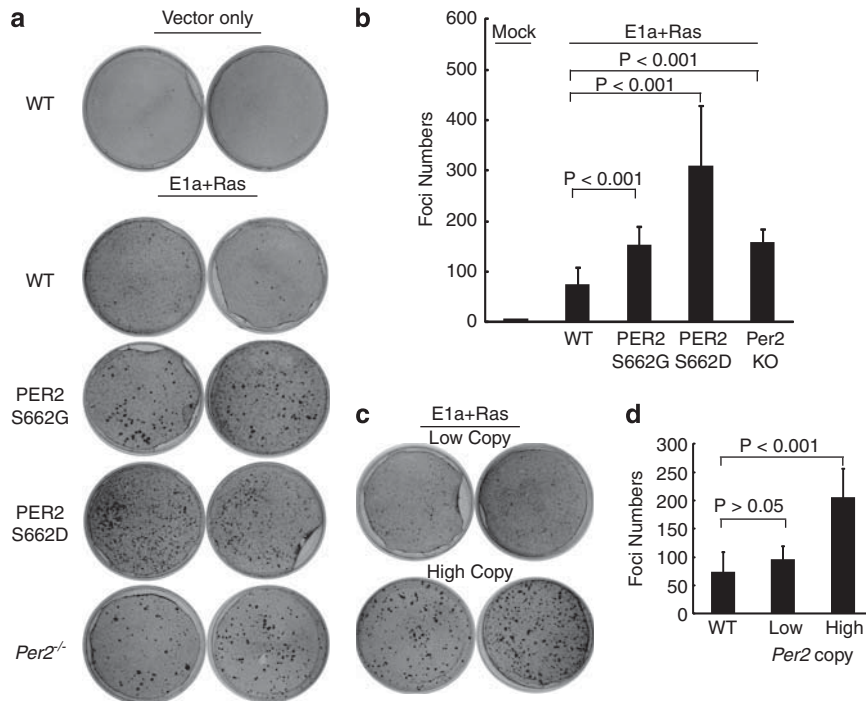


Figure 4 Dysregulation of *PER2* increases formation of oncogenic E1A-RAS-mediated foci in MEFs. (a) and (c) Passage 0 MEFs with the indicated genotypes were infected with retroviruses encoding E1A-RAS. Transfections with empty virus vector were used as negative controls. Two representative culture plates are shown per genotype from at least two repeated independent experiments. (b) and (d) The numbers of foci per 60-mm plate in the assays are expressed as means \pm S.D. ($N = 6$ for each group; one-way ANOVA followed by Dunnett's test)

PER2^{S662G} affects changes in the relative phases of clock-controlled cell cycle gene. To understand the mechanism underlying tumorigenesis, the clock-related cell cycle genes

p21, *c-Myc*, *Cyclin D1* and *p27* were assayed in *Per2* allele mutant MEFs. Unexpectedly, in several independent experiments, the expression levels of these circadian-related

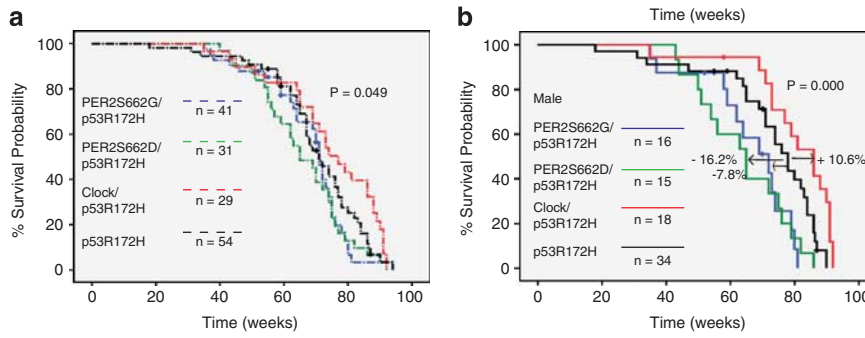


Figure 5 *PER2^{S662}* mutations increased tumor incidence in the *p53^{R172H/+}* background. (a) Overall survival. (b) Male survival. Survival curves (Kaplan–Meier representation) of the indicated mouse cohorts. *n* = number of mice per genotype. The survival curves are plotted with respect to the number of weeks using SPSS software. Statistical significance was assessed using the log-rank test and is indicated (*P*-value). Alterations in median life span of the indicated genotypes relative to control (increase as plus or decrease as minus) are labeled



Figure 6 Female-specific neural tube defects in *p53^{R172H/R172H}* mice. (a) *p53^{R172H/R172H}* female embryos develop exencephaly, which results from a failure of neural tube defects. This is a represent from 13.5-day mouse embryo from *p53^{R172H/+}* and *p53^{R172H/+}* crosses. Two *p53^{R172H/R172H}* females all develop exencephaly (arrow). (b) HE staining for female embryo neural tubes with exencephaly (arrow)

Table 1 Tumor spectrum analysis of *PER2^{S662G2H};p53^{R172H/+}*, *PER2^{S662D2H};p53^{R172H/+}* and *p53^{R172H/+}* mice

Tumor types	<i>p53^{R172H}</i>	<i>PER2^{S662G2H};p53^{R172H}</i>	<i>PER2^{S662D2H};p53^{R172H}</i>
Lymphoma	13/46 (28.2%)	6/33 (18.2%)	7/31 (22.6%)
Osteosarcoma	14/46 (36.1%)	10/33 (30.3%)	9/31 (29.0%)
Fibrosarcoma	7/46 (15.2%)	3/33 (9.1%)	5/31 (16.1%)
Liver tumors	4/46 (8.7%)	9/33 (27.3%)	6/31 (19.4%)
Unknown	2/46 (4.3%)	2/33 (6.1%)	4/31 (12.9%)
Multiple tumors	4/46 (8.7%)	2/33 (6.1%)	4/31 (12.9%)
Metastasis	8/46 (17.4%)	5/33 (15.2%)	4/31 (12.9%)

cell cycle regulators are not significantly different in *Per2* allele mutant MEFs compared with the wild-type (Figure 7 and Supplementary Figure S4). We noticed that *p21* transcripts show peak levels when *Cyclin D* attains trough levels in the wild-type MEFs. However, the relative phases of *p21* and *Cyclin D* appear to be highly similar in these *Per2* allele mutant MEFs in contrast to the wild-type MEFs. It is important to note that *p21* transcript phases are delayed in *Per2* allele mutant MEFs, which may bring changes in the relative phases between *p21* and *Cyclin D* (Figure 7).

For the *p21* gene, it has been described previously that its regulatory region contains a RORE binding site and is regulated by the antagonistic activities of the orphan nuclear receptors NR1D1/2 and NR1F1.²⁴ The question then arises as to whether NR1D1 mediates the *p21* phase shifting. Therefore, we examined the transcription profiles of *Nr1d1* to compare the results obtained from *p21* and *Cyclin D*. We found the accumulation of *Nr1d1* cycles with an antiphase to that of *p21* transcription in the wild-type MEFs, indicating that NR1D1 inhibits the transcription of *p21* expression as

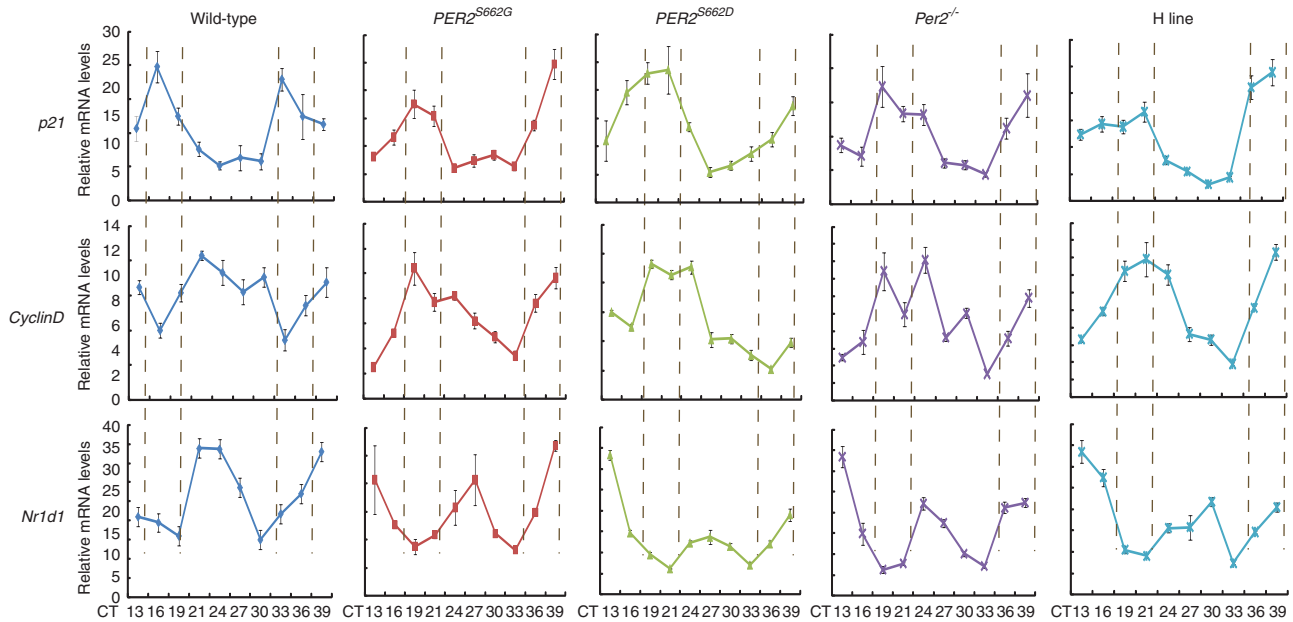


Figure 7 The relative phases of cell cycle genes are shifted by PER2 mutations. Wild-type and different PER2 mutant MEFs were synchronized by a dexamethasone treatment, and RNA was extracted at 3 h intervals starting 10 h after the shock. *p21*, *Cyclin D1* and *Nr1d1* expression analysis were done by q-PCR. Experiments were repeated independently at least three times with consistent results. Plotted values are the mean values \pm S.D. Cosinor analysis was performed on mRNA profiles using SPSS 17.0. The amplitude and acrophase obtained from cosinor analysis were further analyzed by Student's *t*-test. The null hypothesis was rejected at $P < 0.05$

described previously.²⁴ While in these mutant MEFs, *p21* expression profiles are uncoupled at least in part from *Nr1d1* expression (Figure 7), thereby offering the possibility that NR1D1 needs wild-type PER2 to regulate the phase of *p21* expression. In addition, as shown in Figure 7, the cycles of *Nr1d1* transcripts respond to intrinsic circadian period in these mutant MEFs, while the periods of *p21* and *Cyclin D* seem to be fixed 24 h in these mutant MEFs no matter whether they own short or long circadian period. Moreover, the phases of *p21* transcripts delay to the same extent in *Per2* allele mutant MEFs, suggesting that the ability of the circadian control of *p21* expression has been abolished when PER2 is mutated, which is mediated mainly through NR1D1. This assumption is supported by a recent study by Isabelle Schmutz *et al.*⁵ demonstrating that PER2 coordinates circadian output by interacting with NR1D1.

The p21 protein inhibits the activity of cyclin-CDK2 or -CDK4 complexes, and functions as a regulator of cell cycle progression at G1.²⁵ Although the *p21* expression levels in these PER2 mutant MEFs remains comparable to that of wild-type MEFs, the peak of *p21* is locked to the abnormal region that overlaps with the peak of the *cyclin D* phase. It is conceivable that the *p21/cyclin D* interval variations may trigger cell cycle progression.

Discussion

The physiological relevance of the PER2^{S662G} mutation to human cancer. In this study, we provided evidence that the human PER2^{S662G} mutation, which causes the FASPS circadian variant, is also responsible for increased cancer risk. To our knowledge, this represents the first instance of experimental evidence that links a human circadian mutation

to cancer risk. Although the cancer incidence data in FASPS individuals are unavailable owing to scarcity of sampling (one family), a missense mutation in the evolutionarily conserved residue of hPER2 (L823V) has been identified in some human breast cancer samples²⁶ and altered PER2 expression is common in human breast malignancies.^{27,28} By comparing the X-ray-induced apoptosis level and transformation rate among *Per2*^{-/-}, PER2^{S662G}, PER2^{S662D} and PER2 dose-dependent BAC transgenic mice, we suggested that PER2^{S662G} is a dominant negative mutation and PER2^{S662D} gains extra function to prevent apoptosis and increase transformation rate. Interestingly, the functional alternations of PER2^{S662G} and PER2^{S662D} displayed in the aspect of cell cycle are different from that in circadian clock, because PER2^{S662G} mice show shorter circadian period length than *Per2*^{-/-} mice and PER2^{S662D} might elongate the circadian period through increasing PER2 protein level. Furthermore, our data that overexpressing and knockout PER2 both trigger more transformation foci and affect normal apoptosis function suggest that maintaining an optimal level of PER2 is critical to reduce the risk of tumorigenesis. Our functional studies of human variants of PER2, together with unbiased analyses in human cancer by other groups, indicate the importance of PER2 in human tumorigenesis. But the hypothesis that the FASPS mutation increases cancer risk in humans remains to be tested in future.

Impaired gene expression or impaired circadian rhythms? Previous work has demonstrated that the PER2^{S662G} and PER2^{S662D} mutations give rise to completely contrary circadian phenotypes in terms of circadian period, phase and amplitude;¹⁵ thus, we predicted

that the *PER2*^{S662G} and *PER2*^{S662D} mutant mice should have contrary cancer risks if impaired rhythm is the culprit. However, the enhanced cancer risk in both *PER2*^{S662G2H};*p53*^{R172H/+} and *PER2*^{S662D2H};*p53*^{R172H/+} mice strongly suggested that the impaired *PER2* gene, not the impaired circadian rhythm, is responsible for the increased cancer risk in these mice. This observation is further supported by survival data from the *PER2*^{S662D2H};*p53*^{R172H/+} and *Clock*^{Δ19/+};*p53*^{R172H/+} mice, both of which exhibited lengthened circadian periods, but showed highly contrary cancer risks. Interestingly, the 'impaired gene' theory is consistent with the observation from cancer risks in *Cry1*^{-/-};*Cry2*^{-/-} mice^{22,29} and *Clock*^{Δ19} mutant mice.³⁰ In addition, we wish to point out that our experiments share an important similarity with the above-mentioned investigations; all of these experimental systems retain the circadian mutant mice on normal light/dark cycles and subject these mice to entrainment from external time cues. Accordingly, the 'impaired gene' theory may only apply to circadian mutant mice kept in normal light/dark cycles. Circadian disruption is not as intense or detrimental in normal cycles as the disruption experienced by shift workers. In this regard, an important future direction may focus on both the respective contribution and the composite consequence of disrupted circadian genes, as well as disrupted circadian rhythm to cancer risk in persistent phase-shifted schedules.

The cell cycle, circadian clock and relative phase. Recent studies have shown that the circadian clock is coupled to the cell cycle processes through clock-controlled genes, which may contain E-box or ROR elements in their promoters. Somewhat surprisingly, although we found that deregulation of *PER2* has a strong effect on the induced transformation of MEFs and tumorigenesis; the gene expression changes in these clock-controlled genes are less profound in *Per2* allele mutant MEFs. This leads us to think about their phase implication. Although the *Nr1d1* transcripts displayed obvious phase shift and period length changes in these mutant MEFs, *p21* transcripts displayed fixed 24-h-period oscillation with phase delay to the same extent, leading to a similar phase to that of *Cyclin D*. It indicates that in the wide-type MEFs, the opposite phases of *p21* and *Cyclin D* are a result of coordination between circadian clock and cell cycle, with circadian clock adjusting transcription phase of *p21* and the main driver of cell cycle. With the interaction of *PER2*, *NR1D1* may be a critical circadian factor in exerting the phase adjusting function. At present, the physiological significance of the altered phases of these genes is unclear, and the phase shifting cannot explain all the phenotypes that are seen in these mutant mice. It is likely that modifier relative phases between the cycle genes influence features such as the number of transformation foci and the development of the tumor-associated fibroblasts. One of the possibilities comes from interfering with phase locking. Oscillation-based synchrony is the most energy-efficient physical mechanism for temporal coordination. It occurs in many biological systems, including two oscillators of cell division and the circadian phase³¹ or within a cell cycle oscillator through multiple regulatory interactions.³² It is

conceivable that, if phase-coupled *p21* appears at a later phase of the inhibitory cycle while *Cyclin D* remains unchanged, the corresponding inhibition of the CDK complex becomes weak. In other words, if the threshold is reached, CDK activation can initialize unexpected cell cycle progression. It would be interesting, therefore, to investigate the extent to which relative phase changes might affect cell cycle progression, transformation and tumorigenesis.

Materials and Methods

Animals. Mice were observed daily and killed when they showed signs of morbidity or tumor growth in accordance to the Guidelines for Human Endpoints for Animals Used in Biomedical Research. Mice were housed in an Assessment and Accreditation Of Laboratory Animal Care credited SPF animal facility. *PER2*^{S662G5H};*p53*^{R175H/+}, *PER2*^{S662D5H};*p53*^{R175H/+}, *Clock*^{Δ19/+};*p53*^{R175H/+} mice and their littermates were derived from *PER2*^{S662} mutants and *Clock*^{Δ19} mutants³³ by crossing with *p53*^{R175H/+} mice. All mutant animals have been backcrossed for more than 10 generations onto a C57BL/6 inbred background. Low-, middle- and high-copy *PER2* BAC transgenic mice were generated, as described previously.¹⁵ Locomotor activity and activity pattern analyses were performed, as described previously.³⁴

X-ray and flow cytometer. Mice were radiated at the indicated ZT times with a single dose of 6 Gy (100 cGy/min) with a XHA600C Medical Electron Linear Accelerator (Shinva Medical Instrument Co., Ltd, Zibo, Shandong, China). Splenic lymphocytes were isolated at 6 h after irradiation, and red cells were removed using Gey's solution. For flow cytometer analyses, splenic lymphocytes were centrifuged at 1000 r.p.m., and the supernatants were thoroughly removed by aspiration and fixed in 70% ethanol. After incubation with 40 μg/ml propidium iodide and 100 μg/ml RNase at 37 °C for 30 min, the samples were analyzed with a Becton Dickinson FACScan flow cytometer using CellQuest software (Becton Dickinson, Auckland, New Zealand).

Retroviral transfection and focus formation assays. The Plate-E virus packaging cells were transfected with the retroviral vector pMXs carrying the cDNA encoding *E1A* and *Ras* or pMXs with GFP as the control using PEI as the transfection reagent.³⁵ Culture media collected 2 days after transfection were used for infection. MEFs were isolated from 13.5-day embryos as described. P1 MEFs were incubated with fresh virus for 6 h. One day after infection, the medium was replaced with fresh DMEM supplemented with 5% fetal bovine serum and puromycin, and the cells were selected after another 48 h. The infection efficiency was > 95%, as estimated by a control experiment. After selection, the cells were plated at 1 × 10⁶ cells/6 cm² for 14 days. The medium was changed every 2 days. Confluent monolayer cultures with foci were rinsed with phosphate buffered saline (PBS), fixed in 10% formalin and stained with 0.1% crystal violet for 20 min; subsequently, the colonies were scored.

Tumorigenesis. Cohorts of mice were monitored carefully for signs of morbidity or obvious tumor burden. Mice with visible neoplasms around 2 cm in diameter were killed and necropsied. Mice with ill health but no visible neoplasms were monitored carefully for signs of morbidity. Moribund mice or mice that died without signs of morbidity were also necropsied. In most cases, tumor-burdened mice could be identified through necropsy and all tissues with suspected gross lesions or neoplasms were further examined by histopathological examination. Samples were fixed in neutral buffered formalin. Tissues with osseous structure were decalcified with 10% hydrochloric acid. Paraffin sections were prepared and stained with hematoxylin and eosin following standard procedures. Tumor spectrum analysis was performed blindly with the assistance of a clinical pathologist.

Q-PCR and reverse transcription-PCR (RT-PCR). Primers are listed in Supplementary Table 2. All procedures were carried out as previously described.³⁴

Western blotting. Tissue proteins were prepared as described previously using a nuclear extraction kit at the indicated circadian time (Active Motif, Carlsbad, CA, USA). Rabbit anti-cyclin E and anti-PPARα (Santa Cruz Biotechnology, Santa Cruz, CA, USA) were utilized for western blotting according to the manufacturer's suggested protocol.

Statistical analysis. Groups of data are presented as mean \pm S.D. One-way analysis of variance (ANOVA) followed by Dunnett's test or Student's *t*-test was used to determine the statistical significance of difference in measured parameters. Difference was considered significant at $P < 0.05$. Cosinor analysis was performed on mRNA profiles using SPSS 17.0. The amplitude and acrophase obtained from cosinor analysis were further analyzed by Student's *t*-test. The null hypothesis was rejected at $P < 0.05$.

Conflict of Interest

The authors declare no conflict of interest.

Acknowledgements. We thank David Weaver for reading the paper and giving insightful comments. We appreciate JS Takahashi for *Clock* mice and Fu & Ptáček labs for PER2^{S662G} transgenic mice. This work was funded by the National Science Foundation of China, the Distinguished Young Scholar Foundation (30725011 to YX), (10971152 to LY) and Ministry of Science and Technology (2010CB945102 to YX).

1. Lowrey PL, Takahashi JS. Mammalian circadian biology: elucidating genome-wide levels of temporal organization. *Annu Rev Genomics Hum Genet* 2004; **5**: 407–441.
2. Reppert SM, Weaver DR. Coordination of circadian timing in mammals. *Nature* 2002; **418**: 935–941.
3. Young MW, Kay SA. Time zones: a comparative genetics of circadian clocks. *Nat Rev Genet* 2001; **2**: 702–715.
4. Panda S, Antoch MP, Miller BH, Su AI, Schook AB, Straume M *et al*. Coordinated transcription of key pathways in the mouse by the circadian clock. *Cell* 2002; **109**: 307–320.
5. Schmutz I, Ripperger JA, Baeriswyl-Aebischer S, Albrecht U. The mammalian clock component PERIOD2 coordinates circadian output by interaction with nuclear receptors. *Genes Dev* 2010; **24**: 345–357.
6. Fu L, Pelicano H, Liu J, Huang P, Lee C. The circadian gene *Period2* plays an important role in tumor suppression and DNA damage response *in vivo*. *Cell* 2002; **111**: 41–50.
7. Yang X. A wheel of time: the circadian clock, nuclear receptors, and physiology. *Genes Dev* 2010; **24**: 741–747.
8. Gery S, Komatsu N, Baldijyan L, Yu A, Koo D, Koeffler HP. The circadian gene *per1* plays an important role in cell growth and DNA damage control in human cancer cells. *Mol Cell* 2006; **22**: 375–382.
9. Davis S, Mirick DK, Stevens RG. Night shift work, light at night, and risk of breast cancer. *J Natl Cancer Inst* 2001; **93**: 1557–1562.
10. Baan R, Grosse Y, Straif K, Secretan B, El Ghissassi F, Bouvard V *et al*. A review of human carcinogens—Part F: chemical agents and related occupations. *Lancet Oncol* 2009; **10**: 1143–1144.
11. Straif K, Baan R, Grosse Y, Secretan B, El Ghissassi F, Bouvard V *et al*. Carcinogenicity of shift-work, painting, and fire-fighting. *Lancet Oncol* 2007; **8**: 1065–1066.
12. Jones CR, Campbell SS, Zone SE, Cooper F, DeSano A, Murphy PJ *et al*. Familial advanced sleep-phase syndrome: a short-period circadian rhythm variant in humans. *Nat Med* 1999; **5**: 1062–1065.
13. Toh KL, Jones CR, He Y, Eide EJ, Hinze WA, Virshup DM *et al*. An hPer2 phosphorylation site mutation in familial advanced sleep phase syndrome. *Science (New York, NY)* 2001; **291**: 1040–1043.
14. Xu Y, Padiath QS, Shapiro RE, Jones CR, Wu SC, Saigh N *et al*. Functional consequences of a CK1delta mutation causing familial advanced sleep phase syndrome. *Nature* 2005; **434**: 640–644.

15. Xu Y, Toh KL, Jones CR, Shin JY, Fu YH, Ptacek LJ. Modeling of a human circadian mutation yields insights into clock regulation by PER2. *Cell* 2007; **128**: 59–70.
16. Lang GA, Iwakuma T, Suh YA, Liu G, Rao VA, Parant JM *et al*. Gain of function of a p53 hot spot mutation in a mouse model of Li-Fraumeni syndrome. *Cell* 2004; **119**: 861–872.
17. Bae K, Jin X, Maywood ES, Hastings MH, Reppert SM, Weaver DR. Differential functions of mPer1, mPer2, and mPer3 in the SCN circadian clock. *Neuron* 2001; **30**: 525–536.
18. Baylies MK, Bargiello TA, Jackson FR, Young MW. Changes in abundance or structure of the per gene product can alter periodicity of the Drosophila clock. *Nature* 1987; **326**: 390–392.
19. Yang Z, Sehgal A. Role of molecular oscillations in generating behavioral rhythms in Drosophila. *Neuron* 2001; **29**: 453–467.
20. Cook JL, May DL, Wilson BA, Walker TA. Differential induction of cytolytic susceptibility by E1A, myc, and ras oncogenes in immortalized cells. *J Virol* 1989; **63**: 3408–3415.
21. Sherr CJ. Principles of tumor suppression. *Cell* 2004; **116**: 235–246.
22. Ozturk N, Lee JH, Gaddameedhi S, Sancar A. Loss of cryptochrome reduces cancer risk in p53 mutant mice. *Proc Natl Acad Sci USA* 2009; **106**: 2841–2846.
23. Embree-Ku M, Boekelheide K. Absence of p53 and FasL has sexually dimorphic effects on both development and reproduction. *Exp Biol Med (Maywood)* 2002; **227**: 545–553.
24. Grechez-Cassiau A, Rayet B, Guillaumond F, Teboul M, Delaunay F. The circadian clock component BMAL1 is a critical regulator of p21WAF1/CIP1 expression and hepatocyte proliferation. *J Biol Chem* 2008; **283**: 4535–4542.
25. Harper JW, Adami GR, Wei N, Keyomarsi K, Elledge SJ. The p21 Cdk-interacting protein Cip1 is a potent inhibitor of G1 cyclin-dependent kinases. *Cell* 1993; **75**: 805–816.
26. Sjöblom T, Jones S, Wood LD, Parsons DW, Lin J, Barber TD *et al*. The consensus coding sequences of human breast and colorectal cancers. *Science (New York, NY)* 2006; **314**: 268–274.
27. Winter SL, Bosnyan-Collins L, Pinnaduwage D, Andrulis IL. Expression of the circadian clock genes *Per1* and *Per2* in sporadic and familial breast tumors. *Neoplasia* 2007; **9**: 797–800.
28. Chen ST, Choo KB, Hou MF, Yeh KT, Kuo SJ, Chang JG. Deregulated expression of the *PER1*, *PER2* and *PER3* genes in breast cancers. *Carcinogenesis* 2005; **26**: 1241–1246.
29. Gauger MA, Sancar A. Cryptochrome, circadian cycle, cell cycle checkpoints, and cancer. *Cancer Res* 2005; **65**: 6828–6834.
30. Miller BH, McDearmon EL, Panda S, Hayes KR, Zhang J, Andrews JL *et al*. Circadian and CLOCK-controlled regulation of the mouse transcriptome and cell proliferation. *Proc Natl Acad Sci USA* 2007; **104**: 3342–3347.
31. Yang Q, Pando BF, Dong G, Golden SS, van Oudenaarden A. Circadian gating of the cell cycle revealed in single cyanobacterial cells. *Science (New York, NY)* 2010; **327**: 1522–1526.
32. Lu Y, Cross FR. Periodic cyclin-Cdk activity entrains an autonomous Cdc14 release oscillator. *Cell* 2010; **141**: 268–279.
33. King DP, Zhao Y, Sangoram AM, Wilsbacher LD, Tanaka M, Antoch MP *et al*. Positional cloning of the mouse circadian clock gene. *Cell* 1997; **89**: 641–653.
34. Wang X, Tang J, Xing L, Shi G, Ruan H, Gu X *et al*. Interaction of MAGED1 with nuclear receptors affects circadian clock function. *Embo J* 2010; **29**: 1389–1400.
35. Morita S, Kojima T, Kitamura T. Plat-E: an efficient and stable system for transient packaging of retroviruses. *Gene Ther* 2000; **7**: 1063–1066.



This work is licensed under the Creative Commons Attribution-NonCommercial-Share Alike 3.0 Unported License. To view a copy of this license, visit <http://creativecommons.org/licenses/by-nc-sa/3.0/>

Supplementary Information accompanies the paper on Cell Death and Differentiation website (<http://www.nature.com/cdd>)